

2

X-622-69-467

PREPRINT

NASA TM X-63733

REMOTE SENSING OF ATMOSPHERIC OZONE USING THE 9.6 μ REGION

C. PRABHAKARA

SEPTEMBER 1969



- GODDARD SPACE FLIGHT CENTER
GREENBELT, MARYLAND

FACILITY FORM 502	N70-11240	
	(ACCESSION NUMBER)	(THRU)
	32	1
	(PAGES)	(CODE)
TMX-63733	13	
(NASA CR OR TMX OR AD NUMBER)	(CATEGORY)	

Reproduced by the
CLEARINGHOUSE
for Federal Scientific & Technical
Information Springfield Va. 22151

X-622-69-467
Preprint

REMOTE SENSING OF ATMOSPHERIC OZONE
USING THE 9.6μ REGION

C. Prabhakara

September 1969

Goddard Space Flight Center
Greenbelt, Maryland

PRECEDING PAGE BLANK NOT FILLED.

CONTENTS

	<u>Page</u>
ABSTRACT	v
INTRODUCTION	1
METHOD	5
9.6 μ OZONE TRANSMISSION FUNCTIONS	10
RESULTS AND DISCUSSIONS	13
A. Comparisons	13
B. Sensitivity and Consistency	23
ACKNOWLEDGEMENTS	28
REFERENCES	29

PRECEDING PAGE BLANK NOT FILMED

REMOTE SENSING OF ATMOSPHERIC OZONE
USING THE 9.6μ REGION

C. Prabhakara

ABSTRACT

Spectral measurements made by a high resolution Infrared Interferometer Spectrometer (IRIS), aboard the Nimbus III satellite are used to deduce, remotely, the atmospheric ozone. This indirect method depends on the emission and absorption properties of ozone in the 9.6μ region, as well as some gross climatological properties of the vertical ozone profile.

Several IRIS spectra have been analyzed and the corresponding vertical ozone distributions are determined. We have compared some ozone soundings made by chemical sounders with those derived by our indirect method. We find the derived profiles can reproduce the gross features of the observed distribution. The total ozone estimated from the derived profiles compares well with the measured total.

We conclude from this study that the atmospheric total ozone can be determined, with the help of IRIS spectra, over a large part of the globe with an accuracy of better than 10%.

REMOTE SENSING OF ATMOSPHERIC OZONE USING THE 9.6μ REGION

INTRODUCTION

Infrared radiation emanating from the earth and its atmosphere is influenced significantly by the three gases H_2O , CO_2 , and O_3 present in relatively small abundance in the earth's atmosphere. These gases produce easily discernible absorption bands in the emergent spectrum. In Figure 1 we show these bands in a sample spectrum obtained by the Infrared Interferometer Spectrometer (IRIS) aboard the polar orbiting Nimbus III satellite. IRIS has nearly a circular field of view of about 145 km and its spectral resolution is 5 cm^{-1} . This IRIS has obtained numerous spectra over the globe between the 15th of April and the 22nd of July 1969. The main purpose of this paper is to determine atmospheric ozone from these spectra.

Prior to the Nimbus III launching, Sekihara and Walshaw (1969) and also Prabhakara (1969) have examined in detail the feasibility of determining the atmospheric ozone from synthetic satellite spectra in the 9.6μ region. Both these studies emphasize the fact that the information content of the 9.6μ band is meager and that the ozone profile could not be uniquely determined from these spectral data alone. These studies further showed that when we supplement the spectral data with some gross features of the vertical ozone profile it is possible to get good estimates of the total ozone. The meteorological importance of total ozone has been well known for a long time (see for e.g. DOBSON et. al., 1928), and we believe the IRIS spectra will enable us to study the temporal and spatial variations of total ozone on a global scale for the first time. However, the investigation presented here is limited to several case studies over the globe where we were able to get ozone soundings simultaneous with the satellite spectra. The objective is to compare the atmospheric ozone derived by our remote sensing method with the balloon borne ozone sonde observations. Such comparisons will enable us to standardize our 'ozone inversion' technique.

The gross features of the vertical ozone profile needed in our method are extracted from climatological data on the vertical distribution of ozone taken from "Ozone Sonde Observations over North America," Volume 4 (Hering and Borden, 1967). From these data we have obtained the mean vertical distribution and the characteristic patterns (C.P.'s) or empirical orthogonal functions (see for e.g. Holmström, 1963) of the ozone profile up to a height of 32 km. In Figure 2a, we show the mean profile and the first two C.P.'s for low latitudes. Similar information for extra tropical latitudes is presented in Figure 2b.

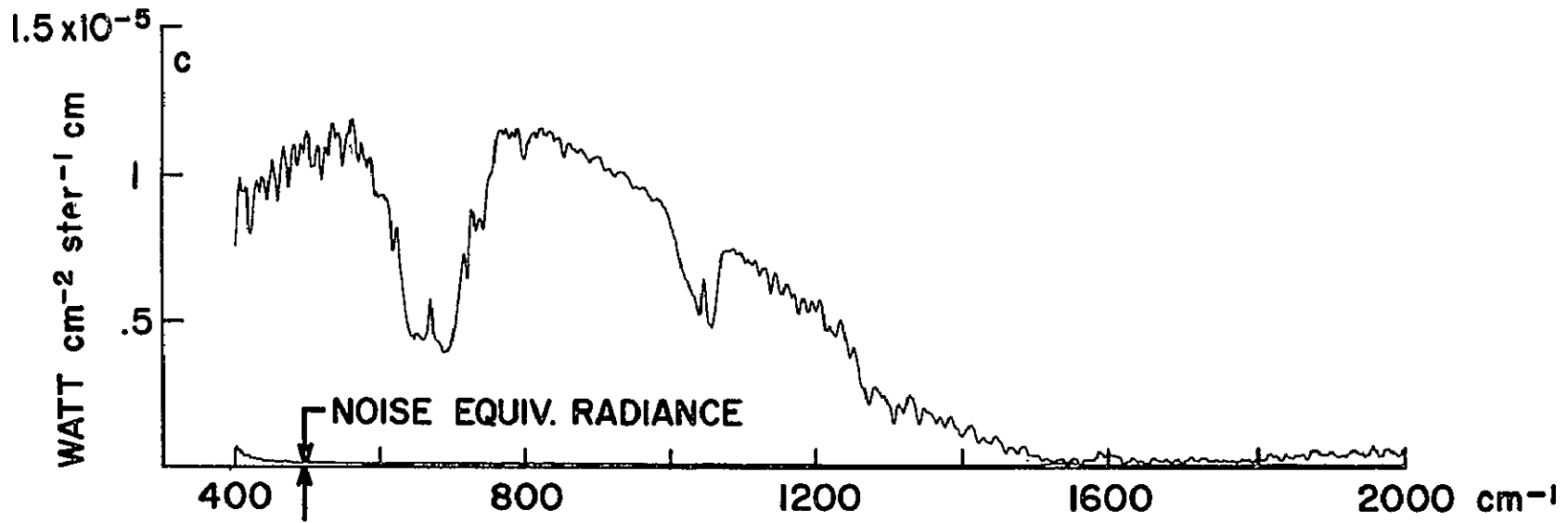


Figure 1—Thermal Emission Spectrum of the Earth Obtained by Infrared Interferometer Spectrometer (IRIS) On-board Nimbus III Satellite

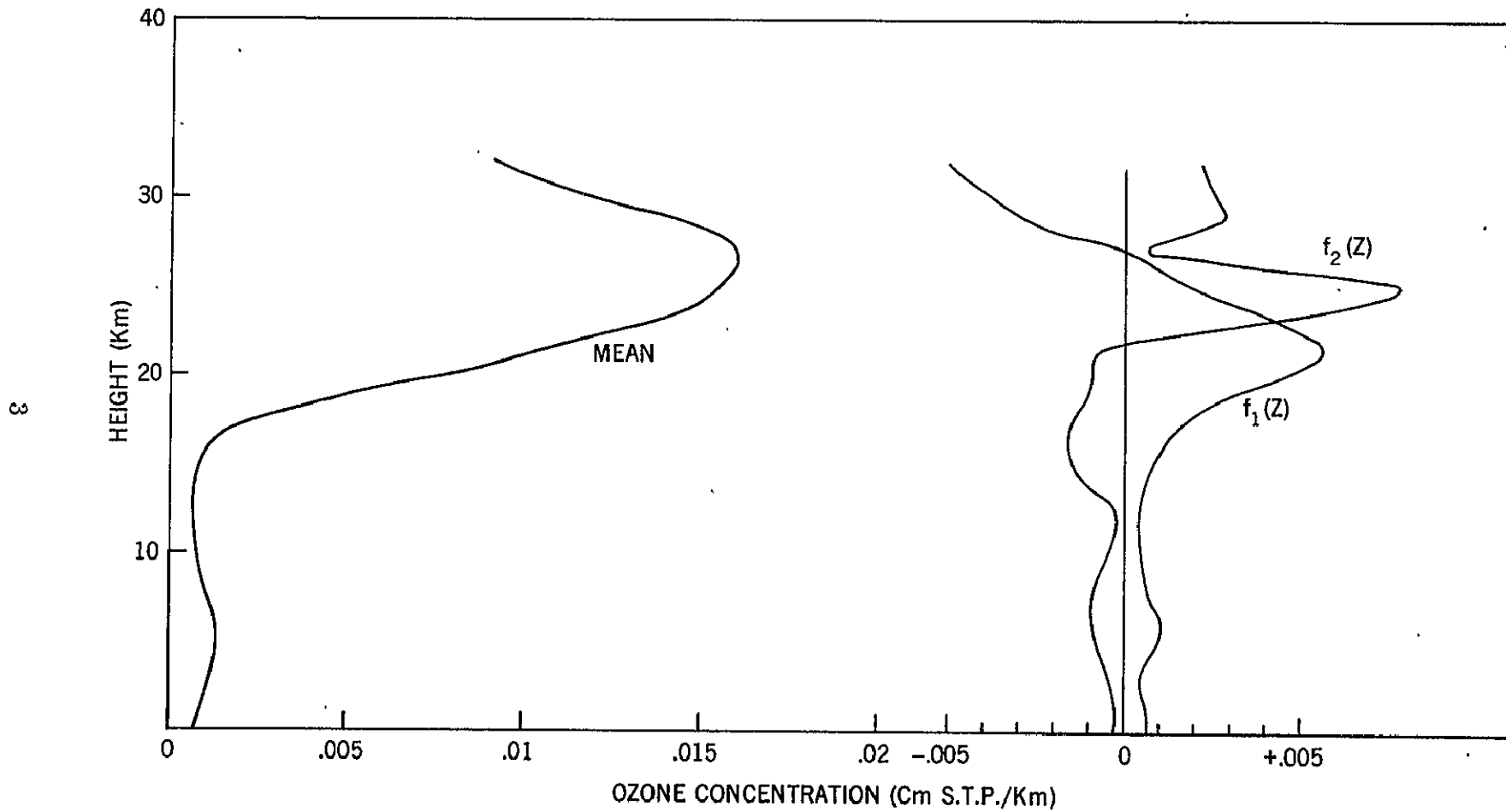


Figure 2a—Mean and the First Two Characteristic Patterns of the Ozone Profile in the Tropical Latitudes

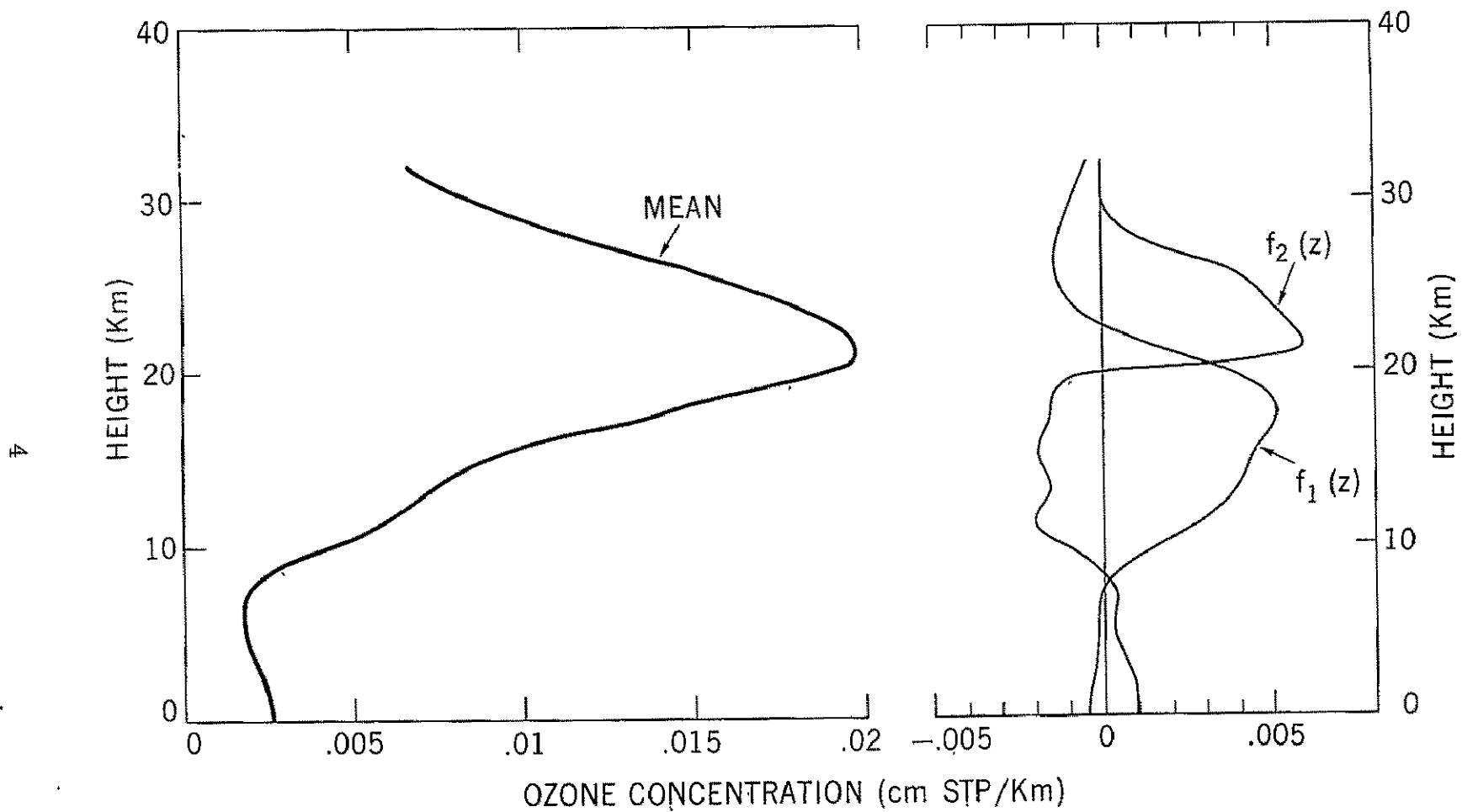


Figure 2b—Mean and the First Two Characteristic Patterns of the Ozone Profile in the Extra-tropical Latitudes

Although we need at least 8 C. P. 's to capture the climatological properties of the ozone profile, we can use only the first C. P. in our inversion method. This limitation arises from the information content of the spectrum in the 9.6μ region. Factor analysis (see for e.g. Mateer, 1965) of several synthetic spectra* reveals the presence of one salient piece of information which can account for about 98% of the variance. Further, the data from IRIS in the 9.6μ region have a random error of about 2%. So a second piece of information may be hard to extract in the presence of "noise" in the spectral measurements. On account of these limitations we have developed a one parameter inversion method which depends on the mean ozone profile and the first C. P. only.

Our results from the several case studies show that the derived ozone profiles from the remote sensing method compare favorably with the chemical ozone sonde profiles. We believe that our technique will yield total ozone accurate to within 10% over most of the globe with the exception of the polar winter zone where conditions of near isothermal temperature distribution can introduce large errors in the inversion method.

METHOD

In a nonscattering atmosphere, if we assume local thermodynamic equilibrium, we can relate the upwelling intensity to the radiative transfer in the atmosphere as follows:

$$I_\nu = B_\nu(T_0) \tau_\nu(0) + \int_{\tau_\nu(0)}^1 B_\nu(T_z) d\tau_\nu(z) \quad (1)$$

where

ν is the wave number,

B_ν is the Planck intensity,

T_0 and T_z are the absolute temperatures at the ground and any height z in the atmosphere, and $\tau_\nu(0)$ and $\tau_\nu(z)$ are the transmissions from ground and any level z to the top of the atmosphere.

*These synthetic spectra were computed changing only the ozone profile while the temperature distribution remained the same.

Equation (1) is basic to all spectrometric remote sensing methods. In the present study, we have suitably adopted this equation to determine the atmospheric ozone from the IRIS measurements in the 9.6μ region.

Obviously, the information regarding the optically active ozone enters equation (1) through the transmission function τ_ν . However, there is also some absorption due to water vapor in the so-called "window" region extending from 8 to 12μ . So the transmission function τ_ν applicable to our study is given by the product of the individual transmissions as shown in equation (2).

$$\tau_\nu(z) = \tau_\nu^{O_3}(z) \cdot \tau_\nu^{H_2O}(z). \quad (2)$$

With the substitution of equation (2) in (1), we have

$$I_\nu = B_\nu(T_0) \cdot \tau_\nu^{O_3}(0) \cdot \tau_\nu^{H_2O}(0) + \int_{\tau_\nu^{O_3}(0)}^1 B_\nu(T_z) \tau_\nu^{H_2O}(z) d\tau_\nu^{O_3}(z) \quad (3)$$

$$\int_{\tau_\nu^{H_2O}(0)}^1 B_\nu(z) \tau_\nu^{O_3}(z) d\tau_\nu^{H_2O}(z).$$

From equation (3) we see that in order to determine ozone we should know the temperature and water vapor distribution present in the atmosphere under the field of view of the instrument. Another important element that we should know and has not been explicitly shown in equations (1) or (3) is the cloudiness. Tropospheric clouds may exist at varying heights and could cover the field of view of the instrument to varying degrees. Although all the information regarding temperature, water vapor, clouds and ozone is contained in the spectra, such as the one shown in Figure 1, the inversion techniques available at present are not capable of extracting the complete information contained in the spectra. Particularly, the cloudy regions of the atmosphere pose a severe problem.

So in the present study we are depending on the data from the radiosonde temperature soundings. The temperature at the surface reported in such soundings is the shelter temperature and is not representative of the true surface temperature present in the field of view. It will be shown later that for the ozone inversion study we need an accurate estimate of the surface temperature. So we determine the effective brightness temperature of the surface from the IRIS

radiance measurements in the region 950 to 980 cm^{-1} adjacent to the 9.6μ band. Ozone has negligible absorption in this spectral region and water vapor has some weak absorption. As a consequence the effective brightness temperature reflects the ground temperature with due allowance for the attenuation of energy by water vapor. Also, when the clouds are present in the field of view, the effective brightness temperature is weighted appropriately by the clear and the cloudy regions. In the following discussion, we will show that by replacing, in equation (3), the true surface temperature by the effective brightness temperature we can eliminate the interaction of both clouds and water vapor.

Since we can neglect the ozone absorption in the region $950 - 980 \text{ cm}^{-1}$ we can define the effective brightness temperature, T_{eff} , for this spectral region in the following way,

$$B(T_{\text{eff}}) = I = B(T_0) \tau_{\text{H}_2\text{O}}^{\text{H}_2\text{O}}(0) + \int_{\tau_{\text{H}_2\text{O}}^{\text{H}_2\text{O}}(0)}^1 B(T_z) d\tau_{\text{H}_2\text{O}}^{\text{H}_2\text{O}}(z). \quad (4)$$

As the spectral measurements have a resolution of 5 cm^{-1} , we can get six estimates of T_{eff} from the spectral interval $950 - 980 \text{ cm}^{-1}$. The average of these six estimates is then taken as the final result. In this manner, we hope to minimize the noise influence.

Now substituting T_{eff} in the place of T_0 we can approximate equation (3) as

$$I_\nu = B_\nu(T_{\text{eff}}) \cdot \tau_{\nu}^{\text{O}_3}(0) + \int_{\tau_{\nu}^{\text{O}_3}(0)}^1 B_\nu(T_z) d\tau_{\nu}^{\text{O}_3}(z). \quad (5)$$

We have used equation (5) in our ozone inversion method.

In order to assess the validity of (5) we show below the residual R obtained by subtracting (5) from (3).

$$R = \left[\int_{\tau_{\text{O}_3}^{\text{H}_2\text{O}}(0)}^1 B(T_z) \tau_{\text{H}_2\text{O}}^{\text{H}_2\text{O}}(z) d\tau_{\text{O}_3}^{\text{O}_3}(z) + \int_{\tau_{\text{H}_2\text{O}}^{\text{H}_2\text{O}}(0)}^1 B(T_z) \tau_{\text{O}_3}^{\text{O}_3}(z) d\tau_{\text{H}_2\text{O}}^{\text{H}_2\text{O}}(z) \right] \\ \left[\int_{\tau_{\text{O}_3}^{\text{O}_3}(0)}^1 B(T_z) d\tau_{\text{O}_3}^{\text{O}_3}(z) + \tau_{\text{O}_3}^{\text{O}_3}(0) \int_{\tau_{\text{H}_2\text{O}}^{\text{H}_2\text{O}}(0)}^1 B(T_z) d\tau_{\text{H}_2\text{O}}^{\text{H}_2\text{O}}(z) \right] \quad (6)$$

Clearly R will be near zero if the layer of the water vapor near the ground is well separated from the ozone layer above. In general, such a condition is obtained in the atmosphere. We will discuss this matter quantitatively in the results and thereby show that equation (5) is a valid approximation to equation (3).

When there are clouds present in the field of view of the instrument the effective brightness temperature is less than the surface temperature reported in the radiosonde temperature data. Further, the energy emitted by the layer of the atmosphere below the clouds is masked. To take these effects into account we make the layer of the atmosphere below the 'clouds' isothermal having a temperature equal to the effective brightness temperature. It can be shown from equation (5) that the emission from such an isothermal layer near the ground is suppressed. The thickness of this layer under the 'clouds' is determined by the height at which the radiosonde temperature is equal to the effective brightness temperature.

The net surface emissivity in the field of view of the instrument also enters implicitly in the definition of the effective brightness temperature. This effective brightness temperature is then assumed to hold true over the entire region 950 to 1070 cm^{-1} . It will be valid, however, only if the water vapor absorption and surface emissivity are constant over the entire spectral interval. We will discuss this matter further in the section on results.

Now we will describe an iterative method to invert the equation (5) in order to retrieve the ozone distribution.

As we had emphasized in the introduction we cannot uniquely determine the ozone distribution from spectral data alone. So additional information such as the gross climatological properties of the ozone profile shown in Figures 2a and 2b are supplied to the inversion method.

We can synthesize an ozone profile as shown in equation (7) by combining the mean ozone distribution, $\bar{O}_3(z)$, and the first C. P., $f_1(z)$.

$$O_3(z) = \bar{O}_3(z) + \alpha_1 f_1(z). \quad (7)$$

The arbitrary constant α_1 in equation (7) constitutes the parameter of the profile. We cannot hope to reproduce all the details of a given ozone profile with just one free parameter. Nevertheless, by this simple procedure some broad features of a given ozone profile could still be simulated and a good match with the total ozone could be obtained. The balloon ozone sonde data yield statistics

of the ozone profile only up to 32 km. Rocket ozone sondes can measure ozone at higher altitudes. But then there are only a limited number of such rocket soundings of ozone (see Krueger, 1969) to yield meaningful statistics. So we have followed a procedure set by the chemical ozone sounders, to extrapolate the ozone profile to higher altitudes. According to this procedure the ozone at higher levels (above about 30 km) is assumed to follow a constant mixing ratio line. Specifically, in our study, we use mixing ratio at 32 km to construct the profile up to 50 km.

Now substituting the model of the ozone profile, which extends to 50 km, in the transmission function we can express the intensity, I_ν , given by equation (5) as a function of the parameter, α_1 , of the ozone profile. In principle we can solve for this parameter and thus get a solution for the ozone profile, if we are given one measurement of intensity in the 9.6μ region. The iterative procedure to do so is given below.

As a first guess let us choose some value for α_1 and then with this guess we can synthesize an ozone profile from equation (7). We can then compute $\tau_\nu(z)$ the transmission in any desired spectral interval. With this transmission and the known temperature distribution we can estimate from equation (5) I'_ν the first guess for the intensity. This calculated intensity in general will be different from the observed intensity I_ν . So we have to determine $\delta\alpha_1$, the adjustment to the parameter α_1 , necessary to match the computed intensity with the observed one. That is done by solving the following equation.

$$\delta I_\nu = (\partial I'_\nu / \partial \alpha_1) \delta \alpha_1 \quad (8)$$

where

$$\delta I_\nu = I_\nu - I'_\nu.$$

The partial derivative $(\partial I'_\nu / \partial \alpha_1)$ is obtained by computing $\partial I'_\nu$, the change in intensity due to a small change $\partial \alpha_1$, in α_1 . When the equation (8) is solved for $\delta \alpha_1$ we can correct our first guess for the parameter α_1 and get an improved guess for the ozone profile. In a similar manner we can make successive iterations until the computed intensity matches the observed one as closely as we wish. The ozone profile computed in this fashion is taken to be the solution.

The one parameter solution requires only one intensity measurement. However, the IRIS spectrum yields with 5 cm^{-1} resolution, 19 spectral measurements, covering the region 980 to 1070 cm^{-1} , which contain information about

ozone. Now since we have no unique way of choosing the particular intensity measurement out of the 19 available to us, we could use all the spectral data in a redundant manner to solve for the one parameter. For this purpose we have adopted a standard method of least squares fitting of the spectral data (e.g., Conrath, 1969). It should, of course, be realized that the least squares fitting of the spectral data in no way guarantees a corresponding agreement of the computed ozone profile with the observed one. However, by this least squares approach we can minimize the influence of noise in spectral measurements.

9.6 μ OZONE TRANSMISSION FUNCTIONS

The transmission functions play a dominant role in all the remote sensing techniques. Slightly spurious set of transmissions can yield significant errors in the inverted solutions. The transmission data derived from theory or laboratory experiment may not have the desired spectral resolution and accuracy. So we may have to apply suitable fine corrections, if possible, to the transmission functions to improve the accuracy of the derived solution. We have followed such a correction procedure in the present study.

The 9.6 μ ozone transmission functions used in this study were synthesized primarily from the studies of Walshaw (1954) and Clough and Kneizys (1965, 1966). Walshaw derived from his experimental investigation the 9.6 μ band model parameters with a resolution of about 6.5 cm⁻¹. On the other hand, Clough and Kneizys resolved the spectrum to about 0.16 cm⁻¹. They were then able to derive the spectral line intensities and positions theoretically, taking into account the Coriolis interaction in the ν_1 and ν_3 fundamentals of ozone. The line intensities and positions resulting from their theoretical study could be used to compute transmission functions over wider spectral intervals. Goldman et al (1967) and also Kunde (1969) have obtained 9.6 μ band parameters in this fashion. The spectral line intensity data of Clough and Kneizys also yields a temperature dependence for such band parameters.

We find that neither Walshaw's data nor the band parameters derived from Clough and Kneizys could explain the observed IRIS spectra satisfactorily. So we have to adjust the band parameters by trial and error until reasonably close agreement with IRIS observations is obtained. We proceed to do so in the following way.

First of all we need a formalism to compute the transmission functions in a nonhomogeneous atmosphere. Such a formalism is adopted from an earlier study of Prabhakara (1969). The transmission τ according to this study is represented as

$$\tau = \text{Exp} - [W_\ell/\delta]. \quad (9)$$

In equation (9) δ stands for the mean line spacing and the equivalent line width W_ℓ is given by

$$W_\ell = \int_{-\infty}^{+\infty} \left[1 - \text{Exp} - \int_z^{\text{Top}} \frac{S}{\pi} \frac{\alpha}{\alpha^2 + (\nu - \nu_0)^2} O_3(z) dz \right] d\nu \quad (10)$$

where S is the mean line intensity

α is the half width of the spectral lines

O_3 is the ozone concentration and ν_0 is the line center.

The half width α is expressed as a function of pressure p and temperature T in the atmosphere.

$$\alpha = \alpha^0 \left(\frac{P}{p^0} \right) \left(\frac{T^0}{T} \right)^{1/2} \quad (11)$$

Here $p^0 = 1$ atm, $T^0 = 273.2^\circ\text{K}$ and $\alpha^0 = 0.073$, a value derived from Walshaw's study.

Further the line intensity S in equation (10) is represented as a function of temperature.

$$S = S^0 \left(\frac{T^0}{T} \right)^{3/2} \text{Exp} - \left[1.439 \cdot E'' \left(\frac{1}{T} - \frac{1}{T^0} \right) \right] \quad (12)$$

In equation (12), E'' is some effective mean estimate of the lower state energy. E'' for each of the 5 cm^{-1} wide spectral intervals, shown in Table 1, is calculated from Clough and Kneizys' data.

S^0 the mean line intensity at standard temperature T^0 and the mean line spacing δ are very essential band parameters. These two parameters were synthesized, by trial and error calculation of intensity, to match some selected IRIS spectra for which we could also get balloon soundings of ozone and temperature up to about 30 km. The S and δ values of Walshaw, and Clough and

Kneizys were used as helpful guidelines in these trial and error calculations. In Table 1 we have listed the values of S and δ derived in the manner described above.

As an independent check on all the band parameters, S, δ , and E'' shown in Table 1, we have performed inversion on several IRIS spectra and obtained a satisfactory matching of both the observed spectrum and the ozone profile. Particularly, the total ozone values derived from these 'ozone inversions' correspond quite well with the observed values. We will be able to discuss these matters quantitatively in the section on results.

It should be emphasized that the band parameters shown in Table 1 were derived by following the formalism of equations (9) through (12) to compute the transmission. However, if a different band model were used these parameters may not adequately reproduce the spectrum.

Table 1
Ozone 9.6 μ Band Parameters

Wave No.	S	δ	S/ δ	E''
980	.004	.106	.038	720
985	.01	.106	.094	720
990	.027	.106	.254	720
995	.071	.106	.67	720
1000	.1086	.082	1.324	720
1005	.1548	.073	2.12	624
1010	.2668	.0706	3.78	507
1015	.3610	.0776	4.65	395
1020	.4830	.0847	5.70	298
1025	.5690	.0882	6.45	210
1030	.5250	.0876	5.99	136
1035	.241	.0435	5.54	145
1040	.233	.0588	3.96	163
1045	.223	.0729	3.059	39
1050	.497	.0565	8.796	114
1055	.597	.0623	9.583	192
1060	.425	.0694	6.123	338
1065	.192	.0647	2.968	582
1070	.016	.060	0.267	857

RESULTS AND DISCUSSIONS

A. Comparisons

There are few balloon-ozone-sounding stations over the globe compared to radio-sonde stations. Further ozone soundings are not made on a daily basis. Due to this reason we could not get a large number of balloon-ozone-soundings coincident, in geographic location and time, with the satellite spectra. So we had to allow considerable margin in time and distance in order to compare the balloon soundings with the ozone profiles derived from spectra. In this manner we could get 5 cases to make a comparative study. In Table 2 we have the information about the time and location of the balloon soundings and IRIS spectra.

Table 2
Time and Position of Balloon Sounding vs IRIS Sounding

Station	Geographic Position	Co-ordinates of IRIS View	Date and Time of Balloon Sounding	Date and Time of Satellite Passage	Orbit No.
Point Mugu	34°07'N 119°07'W	34°N 118°W	June 28, '69 1753Z	June 28, '69 1852Z	1012
Point Mugu	34°07'N 119°07'W	34°N 116°W	July 8, '69 2215Z	July 8, '69 1844Z	1146
Potsdam	52°23'N 13°03'E	52°N 11°E	June 11, '69 0700Z	June 11, '69 0952Z	779
Goose Bay	53.3°N 60.4°W	53°N 63°W	May 22, '69 1200Z	May 23, '69 1447Z	527
Aspendale	38°02'S 145°06E	38°S 147°E	April 21, '69 1202 EST	April 20, '69 1205Z	83
Grand Turk	21.5°N 71.1°W	21°N 71°W	April 30, '69 1130Z	May 1, '69 0431Z	226
Balboa	9°N 79.6°W	9°N 82°W	April 16, '69 1115Z	April 18, '69 1635Z	59

In addition to the 5 cases mentioned above, we had organized 2 balloon soundings from Point Mugu (California) (see Table 2) concurrent with the Nimbus III passage. The present study of remote sensing of ozone is based on these 7 cases.

We have used the two Point Mugu soundings shown in Figures 3 and 4 for the determination of S and δ , following the scheme outlined earlier. Then with these band parameters we performed inversion on the same cases using the representation of the ozone profile given by the statistics shown in Figure 2b. The recovered profiles are able to reproduce the salient features of the distribution quite well. The derived total ozone in the two cases agrees within 4%.

We have then performed inversion at the remaining 5 stations. These computed ozone profiles are compared with the corresponding balloon soundings in Figures 5 to 9. The computed spectral intensities are also compared in Table 3 with the corresponding IRIS measured intensities. The intensities are reproduced very well in all the cases. We therefore feel the band model parameters are properly chosen.

Since we cannot expect more than a qualitative agreement between the observed and computed ozone profiles we will consider total ozone as a quantitative measure to compare. The computed total ozone is within about 10% of the observed total for the three stations Aspendale (Australia), Potsdam (Germany) and Goosebay (Canada) where in addition to the chemical soundings simultaneous measurement of total ozone by 'Dobson' instrument is also available. The 'Dobson' measured totals are used to standardize the chemical sounding. So the comparison for these three cases is quantitative.

The seasonal changes in total ozone and ozone profile near the equator are small. (See Figure 2 of Hering and Borden, 1965). So we believe the comparative study made for Balboa and Grand Turk is meaningful despite poor synchronization of time.

We are not able to quantitatively compare with several other chemical ozone soundings as they were not standardized by Dobson measurements. The chemical ozone soundings often require a correction to yield total ozone in agreement with 'Dobson' measurements (Mueller, 1968). Such a correction is made by multiplying the ozone concentration, at all points in the sounding, by one correction factor. When such a correction factor based on 'Dobson' measurement is not available an educated guess is made to give a correction factor. We have no way of assessing the accuracy of a guess. This is mainly the reason for our inability to quantitatively compare those cases where 'Dobson' reading is absent.

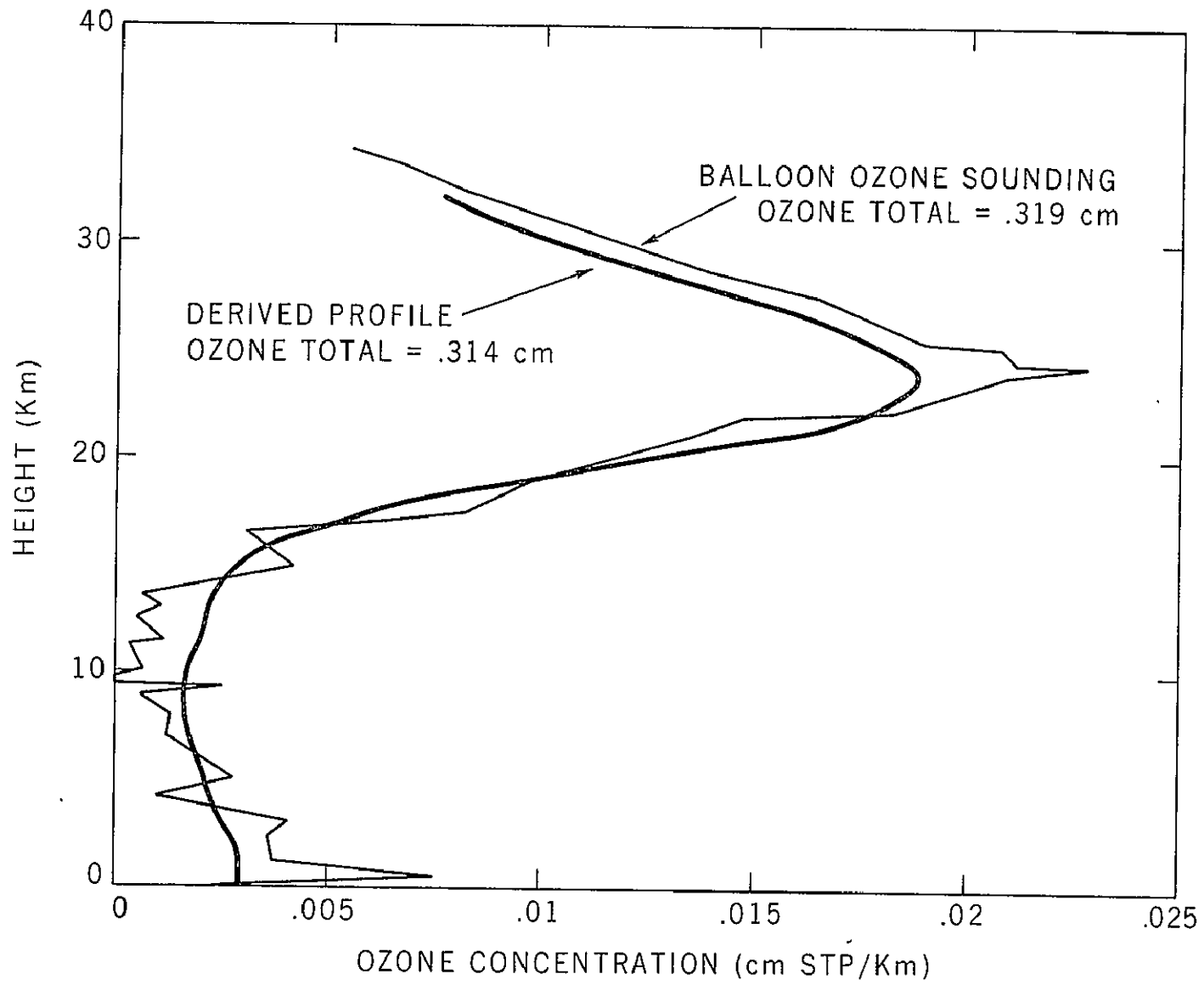


Figure 3—Ozone Inversion for the Case of Point Mugu (California), Orbit 1012, June 28, 1969

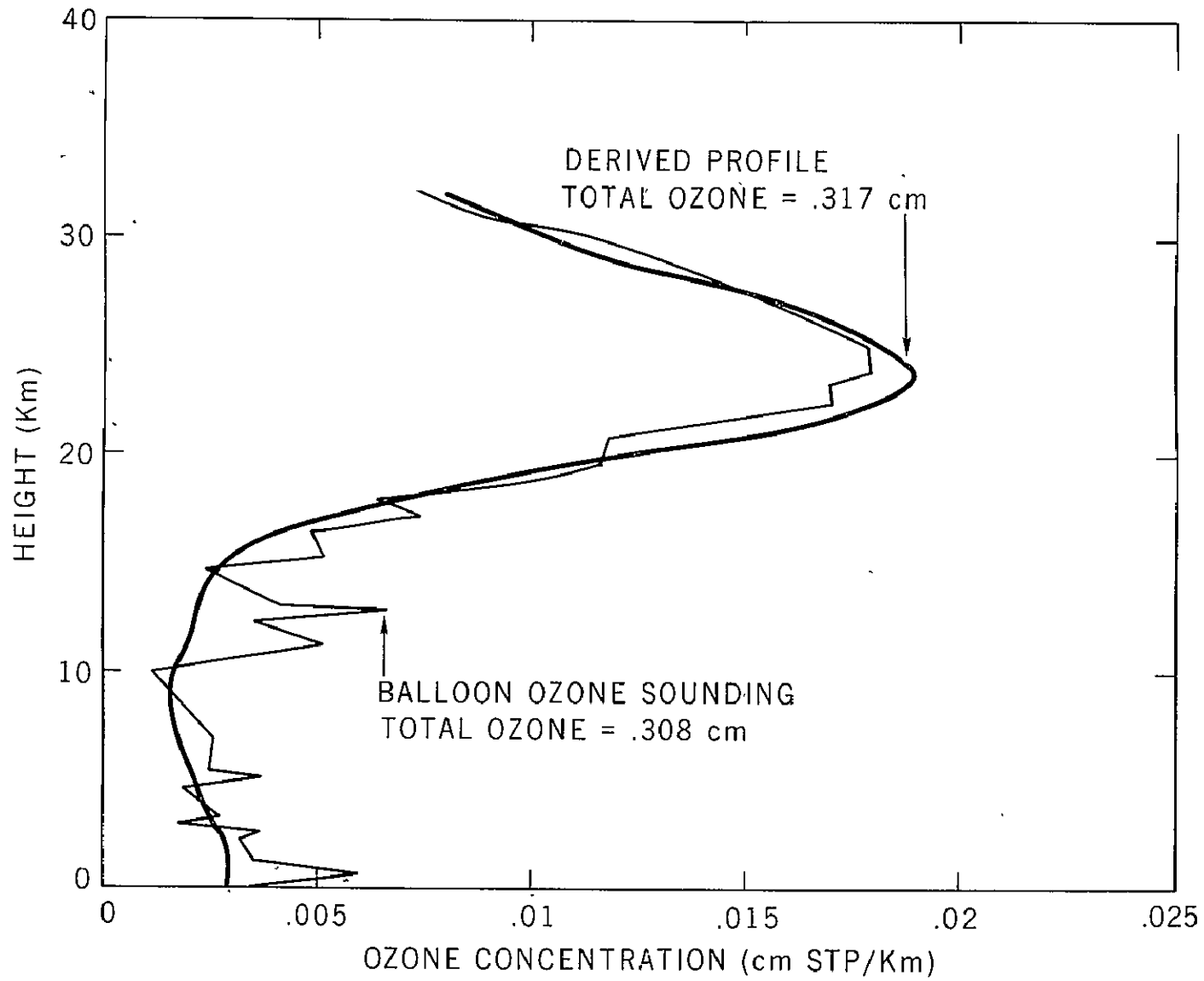


Figure 4—Ozone Inversion for the Case of Point Mugu (California), Orbit 1146, July 8, 1969

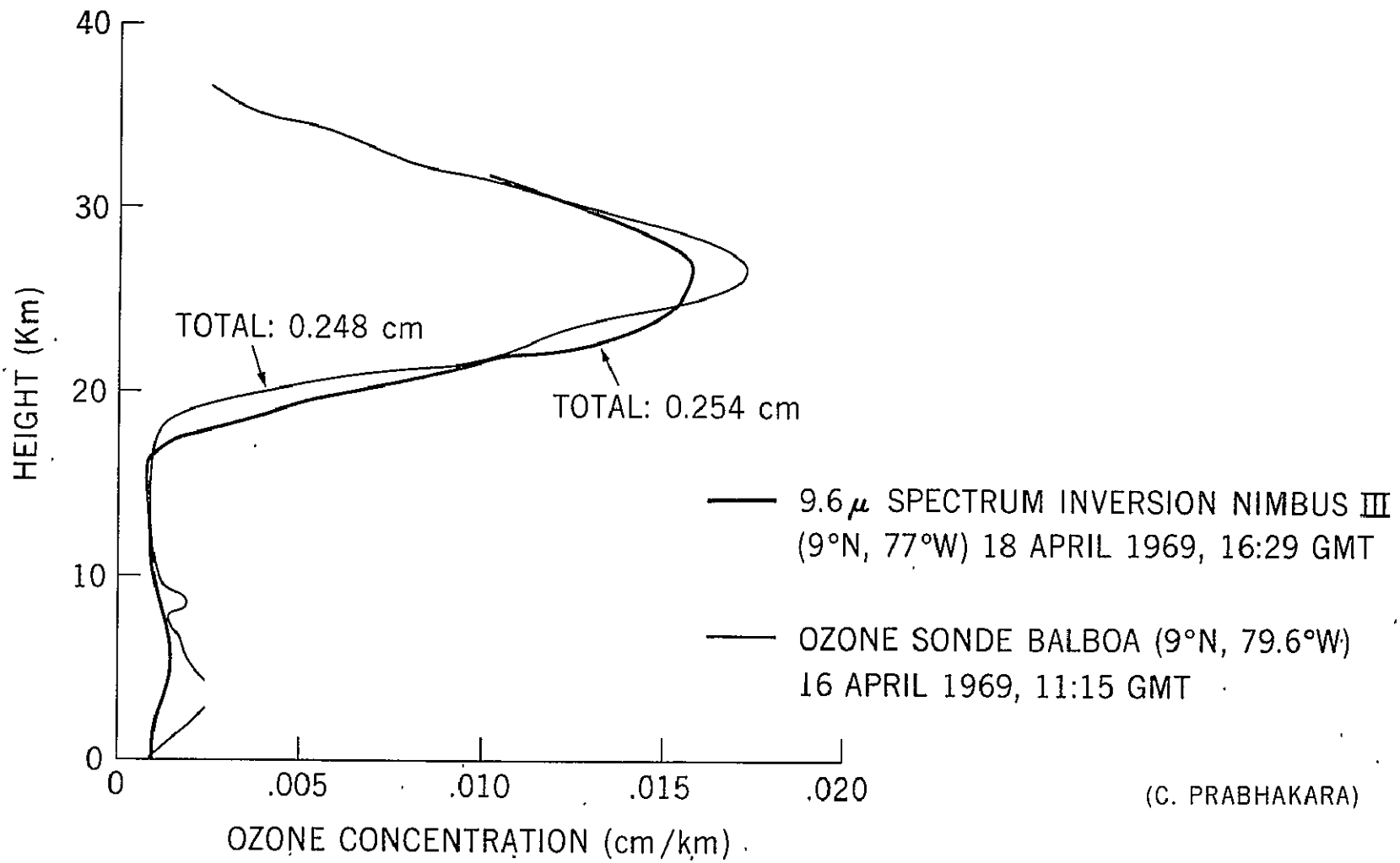


Figure 5—Ozone Inversion for the Case of Balboa (Canal Zone), April 18, 1969

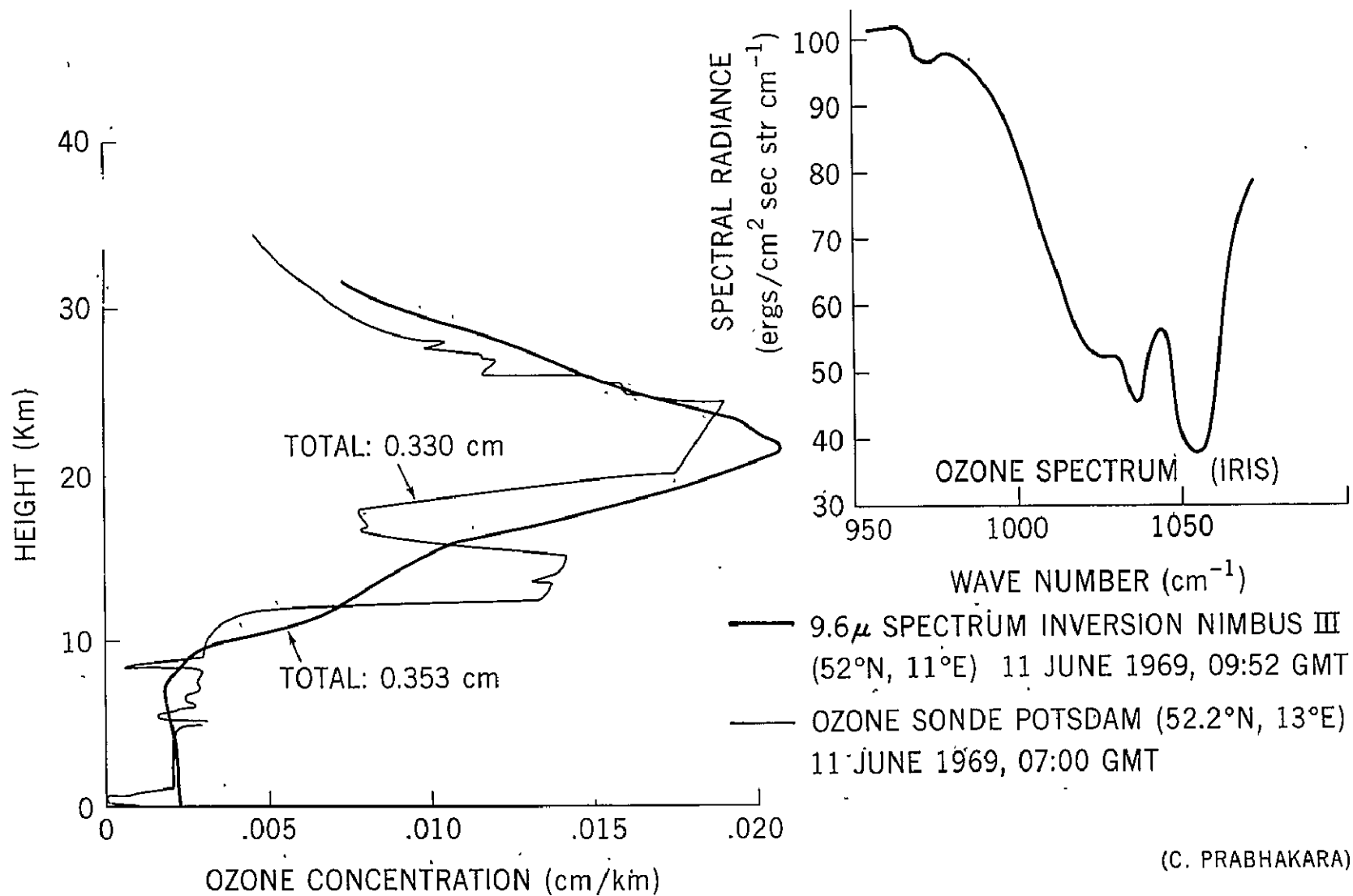


Figure 6—Ozone Inversion for the Case of Potsdam (Germany), June 11, 1969

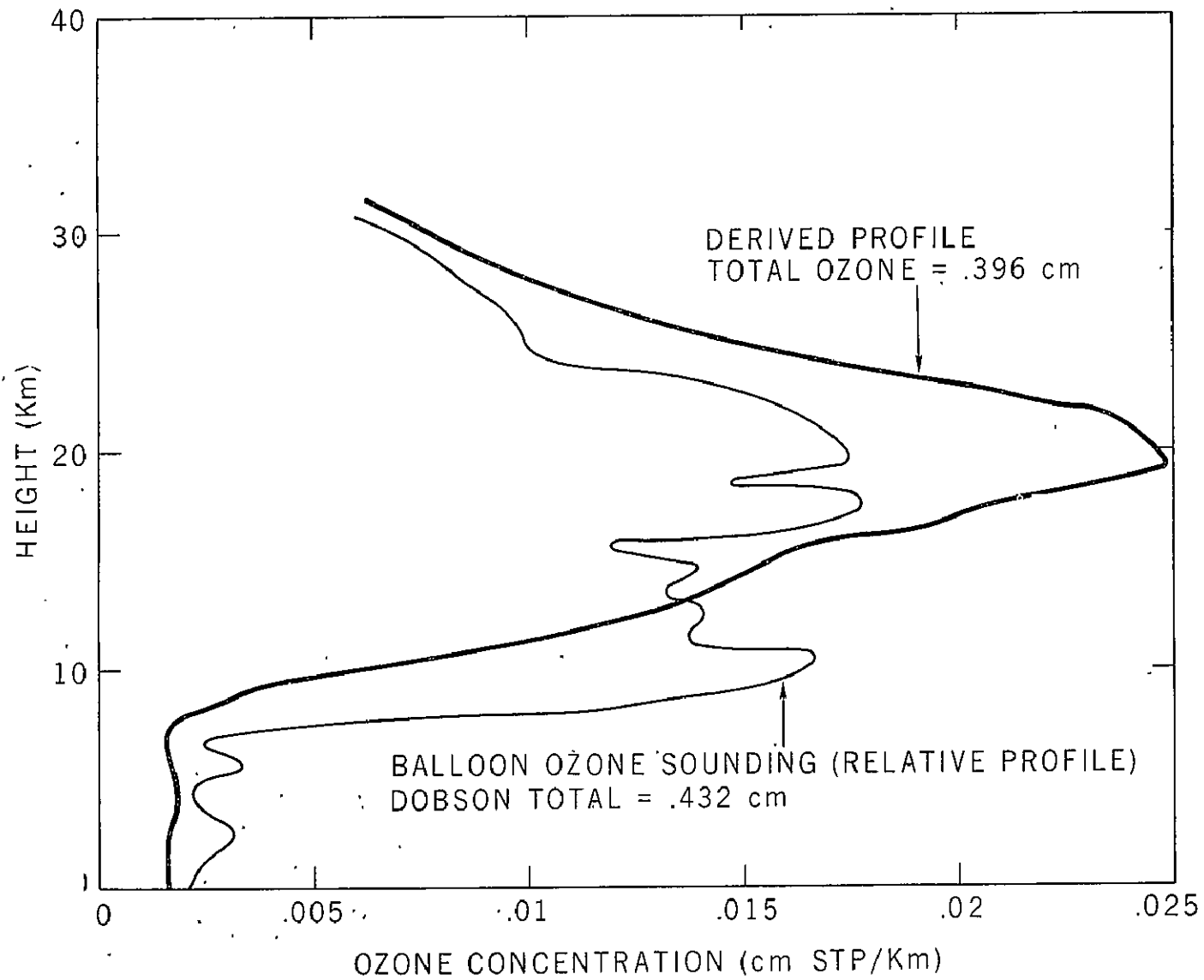


Figure 7--Ozone Inversion for the Case of Goose Bay (Canada), May 23, 1969

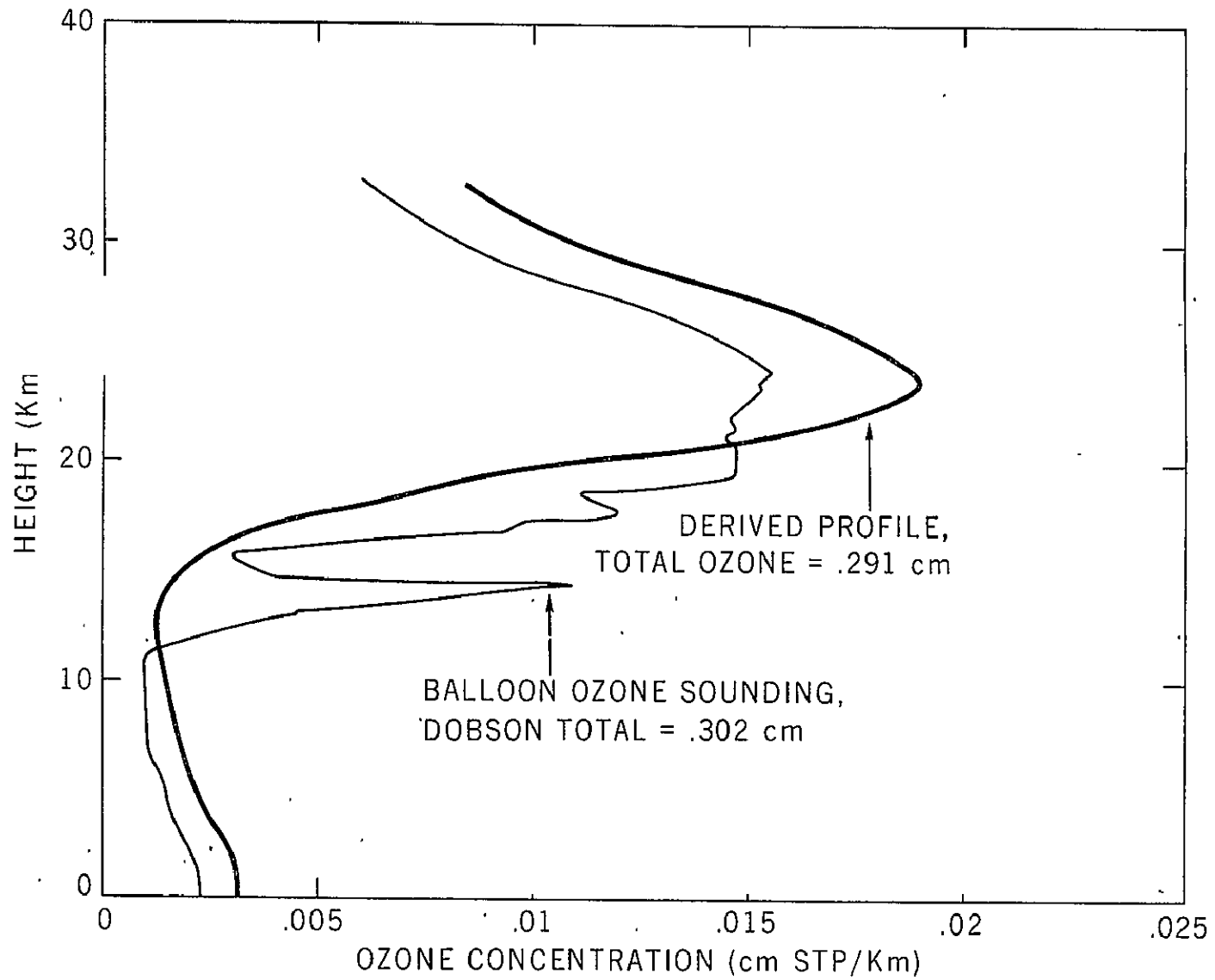


Figure 8—Ozone Inversion for the Case of Aspendale (Australia), April 20, 1969

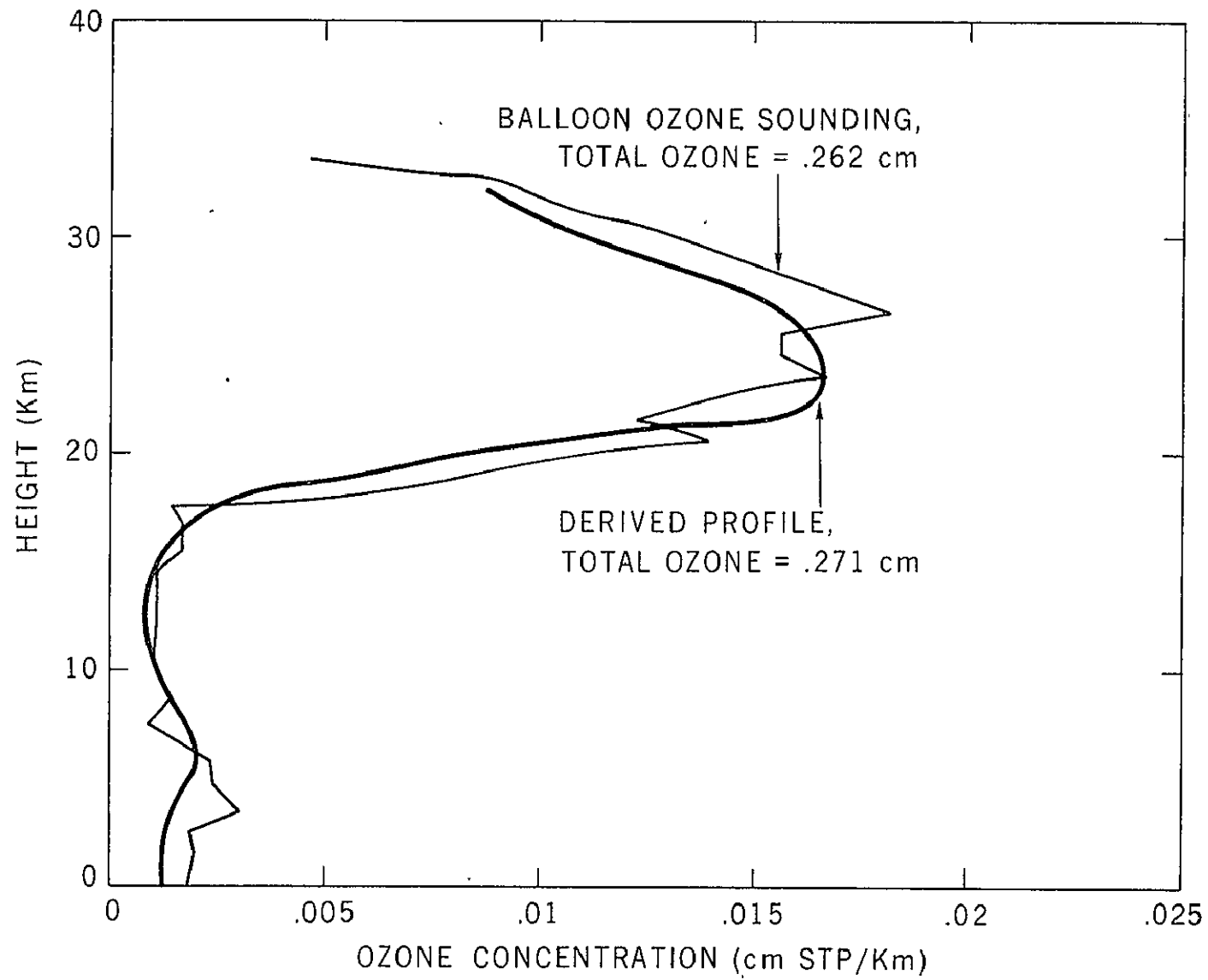


Figure 9—Ozone Inversion for the Case of Grand Turk (Bahamas), May 1, 1969

Table 3
Comparison Between Radiance Measured (IRIS) and Computed (C)

Wave No.	Point Mugu #1012		Point Mugu #1146		Potsdam		Goose Bay		Aspendale		Grand Turk		Balboa	
	Iris	C	Iris	C	Iris	C	Iris	C	Iris	C	Iris	C	Iris	C
980	105.9	104.4	130.4	129.6	97.12	95.85	67.55	68.02	76.84	75.16	76.63	76.06	69.45	70.34
985	103.9	102.8	128.3	127.6	95.14	94.19	67.58	66.75	76.29	73.93	74.90	74.89	69.40	69.27
990	100.3	100.2	126.2	124.3	91.73	91.47	64.41	64.71	73.79	72.15	74.05	73.20	67.5	67.80
995	96.00	96.02	121.6	119.0	89.40	87.06	60.17	61.38	71.35	69.68	71.50	70.76	65.7	65.74
1000	90.32	90.84	113.8	112.2	82.13	81.54	57.64	57.29	67.93	66.20	69.64	67.78	62.8	63.24
1005	84.84	84.65	105.7	104.0	75.59	74.85	52.52	52.47	63.97	62.28	65.40	64.18	60.2	60.25
1010	77.74	75.65	94.04	91.86	67.53	65.23	47.47	45.85	56.27	56.65	60.00	58.98	55.9	55.97
1015	71.28	71.00	84.72	85.67	59.86	60.36	42.85	42.65	54.17	53.61	56.00	56.03	51.8	53.47
1020	64.84	66.50	79.06	79.69	53.81	55.79	39.01	39.73	51.32	50.65	52.4	53.12	49.9	50.99
1025	63.09	62.78	75.6	74.80	51.94	52.12	37.48	37.41	47.35	48.16	50.9	50.62	49.00	48.81
1030	61.89	61.56	73.8	73.34	52.28	50.92	35.92	36.61	46.38	47.19	49.0	49.53	47.93	47.81
1035	54.83	55.09	63.97	64.76	44.87	45.05	31.52	32.68	42.00	43.03	44.9	45.32	43.8	44.20
1040	60.56	62.65	73.35	75.28	52.30	52.18	36.80	37.01	46.31	47.49	48.35	49.65	47.0	44.71
1045	63.56	64.82	76.24	78.42	54.52	54.24	36.82	38.37	48.20	48.58	51.27	50.49	48.13	48.30
1050	49.00	48.67	56.09	56.19	39.34	39.11	27.50	28.88	38.94	38.48	40.9	40.82	39.35	40.14
1055	48.99	49.43	57.16	57.66	37.90	40.02	28.78	29.23	39.66	38.97	41.7	41.45	40.39	40.62
1060	59.75	59.13	70.78	71.17	47.25	49.13	35.40	34.50	44.37	44.79	46.0	47.21	49.6	45.35
1065	74.75	70.83	92.59	87.58	63.86	61.44	46.79	42.17	53.74	51.69	54.9	53.66	52.4	50.48
1070	85.2	86.09	105.4	108.7	76.05	78.13	53.93	53.82	58.46	60.41	60.1	61.35	56.8	56.47

At the present time we have only a few quantitative comparisons which indicate an agreement to within 10% on the total ozone. We believe several more quantitative comparisons are necessary to assess the accuracy of our method.

In Table 4 we have compared the measured and derived total ozone for all the cases (see Table 2)

Table 4
Total Ozone Comparison

Station	Observed Total Ozone (cm STP)	Computed Total Ozone (cm STP)
Point Mugu #1012	.319	.314
Point Mugu #1146	.308	.317
Potsdam	.330*	.353
Goose Bay	.432*	.396
Aspendale	.302*	.291
Grand Turk	.262	.271
Balboa	.248	.254

*Total ozone measured by Dobson instrument.

B. Sensitivity and Consistency

In this Section we will try to demonstrate the sensitivity of the derived solution to the input information. Such an insight helps to establish the internal consistency and the inherent capability of our method.

The basic input information for any given ozone inversion is the temperature distribution in the atmosphere and the IRIS radiance measurements in the region 950 to 1070 cm^{-1} . Any errors present in these data will propagate into the derived solution.

The 'noise equivalent radiance' of IRIS spectral measurements (in the region 950 to 1070 cm^{-1}) is about 2 $\text{ergs/cm}^2 \text{sec} \cdot \text{ster} \cdot \text{cm}^{-1}$. However, since we use these radiance measurements in a highly redundant fashion we expect to minimize the influence of such errors.

The input temperature distribution often does not match closely in time and geographic location to the IRIS spectrum. So the true temperature distribution in the field of view of IRIS could be slightly different. It will be desirable to determine the atmospheric temperature distribution in a consistent fashion from IRIS measurements in the 15μ region. At present we determine only the effective brightness temperature of the surface from the measured radiance.

In order to bring out the sensitivity of our method to the temperature distribution in the atmosphere and the effective brightness temperature of the surface we are presenting the following analysis.

First let us consider the weighting function $d\tau/dz$. In Figure 10 we have presented two weighting functions, one centered at 1000 cm^{-1} and another at 1050 cm^{-1} , for the case of Potsdam. These two spectral intervals, a weak one at 1000 cm^{-1} and a strong one at 1050 cm^{-1} , can describe adequately the behavior of the entire 9.6μ band. The weighting functions are very similar and closely resemble the ozone profile. An analogous result is found in an independent study made by Sekihara and Walshaw (1969). It is for this reason the entire 9.6μ spectrum contains one dominant piece of information.

The simplicity and close similarity of the weighting functions permits us to approximate the radiative transfer equation to a good degree of accuracy in the following form.

$$\begin{aligned}
 I_{\nu} &= B_{\text{eff}} \tau_{\nu}(0) + \int_{\tau_{\nu}(0)}^1 B d\tau \\
 &\cong B_{\text{eff}} \tau_{\nu}(0) + \bar{B} [1 - \tau_{\nu}(0)].
 \end{aligned}
 \tag{13}$$

Where \bar{B} is some weighted mean temperature defined as

$$\bar{B} = \frac{\int_{\tau_{\nu}(0)}^1 B d\tau}{\int_{\tau_{\nu}(0)}^1 d\tau_{\nu}}.
 \tag{14}$$

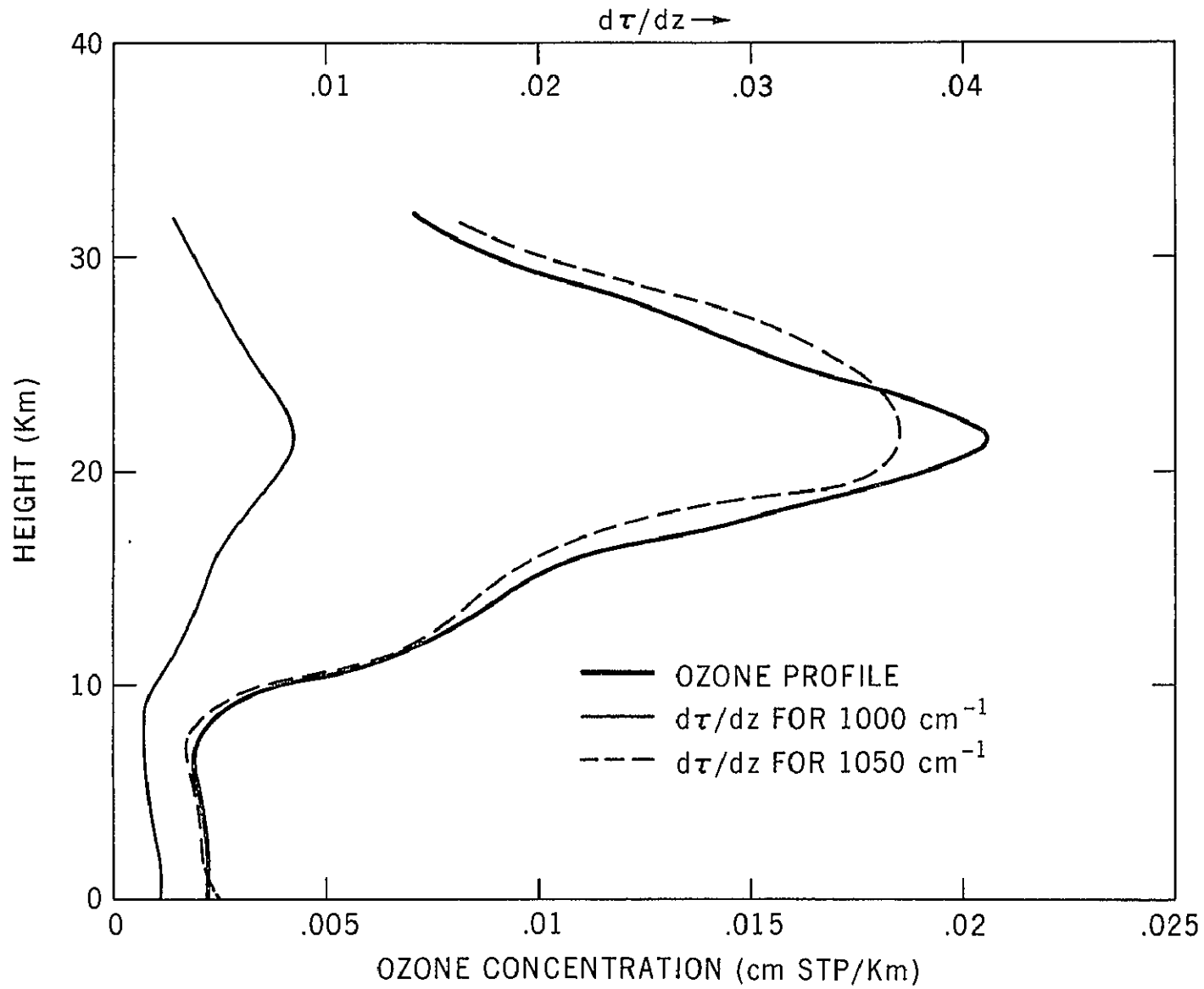


Figure 10—Computed Ozone Profile for Potsdam (June 11, 1969) and the Weighting Functions $d\tau/dz$ for the two spectral intervals, 5 cm^{-1} wide, Centered at 1000 cm^{-1} and 1050 cm^{-1}

Now since the weighting functions for all the spectral intervals in the 9.6μ region are similar, \bar{B} given by equation (14) varies very little as a function of wave number. The relative importance of the effective brightness temperature of the surface and the temperature distribution in the atmosphere can be discussed readily with the help of equation (13).

The first term on the right hand side of equation (13), $B_{\text{eff}} \tau_{\nu}(0)$, is the energy transmitted from the surface to the top while the second term, $\bar{B} [1 - \tau_{\nu}(0)]$ is the emission from the whole atmosphere. The two terms together contribute to the intensity reaching the top of the atmosphere. In order to illustrate the relative importance of these two terms we have plotted them as a function of wave number in Figure 11 for the case of Potsdam. The intensity I_{ν} and the transmission τ_{ν} are also shown in the same figure. We cannot fail to notice the similarity of the curves denoted I_{ν} , $B_{\text{eff}} \tau_{\nu}(0)$, and $\tau_{\nu}(0)$. The curve showing emission, $\bar{B} [1 - \tau_{\nu}(0)]$, bears inverse relationship with respect to the other three curves in the same figure. It is readily seen that $B_{\text{eff}} \tau_{\nu}(0)$ is overweighing the term $\bar{B} [1 - \tau_{\nu}(0)]$ over the entire band. However, in the strong regions of the band the two terms approach one another. The preceding discussion establishes the importance of the effective brightness temperature of the surface. Since we are determining this temperature from the IRIS data we expect to have a minimal error introduced into our solution by the term $B_{\text{eff}} \tau_{\nu}(0)$.

Now let us consider what happens if the temperature in the atmosphere is increased, say by 10°C . From equation (13) we will expect $\bar{B} [1 - \tau_{\nu}(0)]$ to increase and $B_{\text{eff}} \tau_{\nu}(0)$ to decrease so as to maintain the intensity at the same value. This will happen only if τ_{ν} decreases, which implies the ozone content in the atmosphere should increase. Actually we find a 10°C increase in temperature at all the points in the atmosphere resulted in about 10% increase in the total ozone estimated for Potsdam. This result reveals the sensitivity of our solution to the input temperature information.

Let us now consider the shape of the computed ozone profile. The derived profile is not always in close agreement with the observed profile. From the foregoing discussion we can see that the total ozone derived will be in error on account of this reason. The only way to assess the magnitude of this error is from several quantitative comparisons and so we will reconsider this issue in a later investigation.

The interaction of the water vapor was eliminated (see equations 5 and 6) by considering an effective mean surface brightness temperature. To test the validity of this approach we have made a controlled test. In this test a synthetic spectrum of the 9.6μ region was computed for a given temperature, water vapor and ozone distribution. The transmission functions of water vapor, needed in

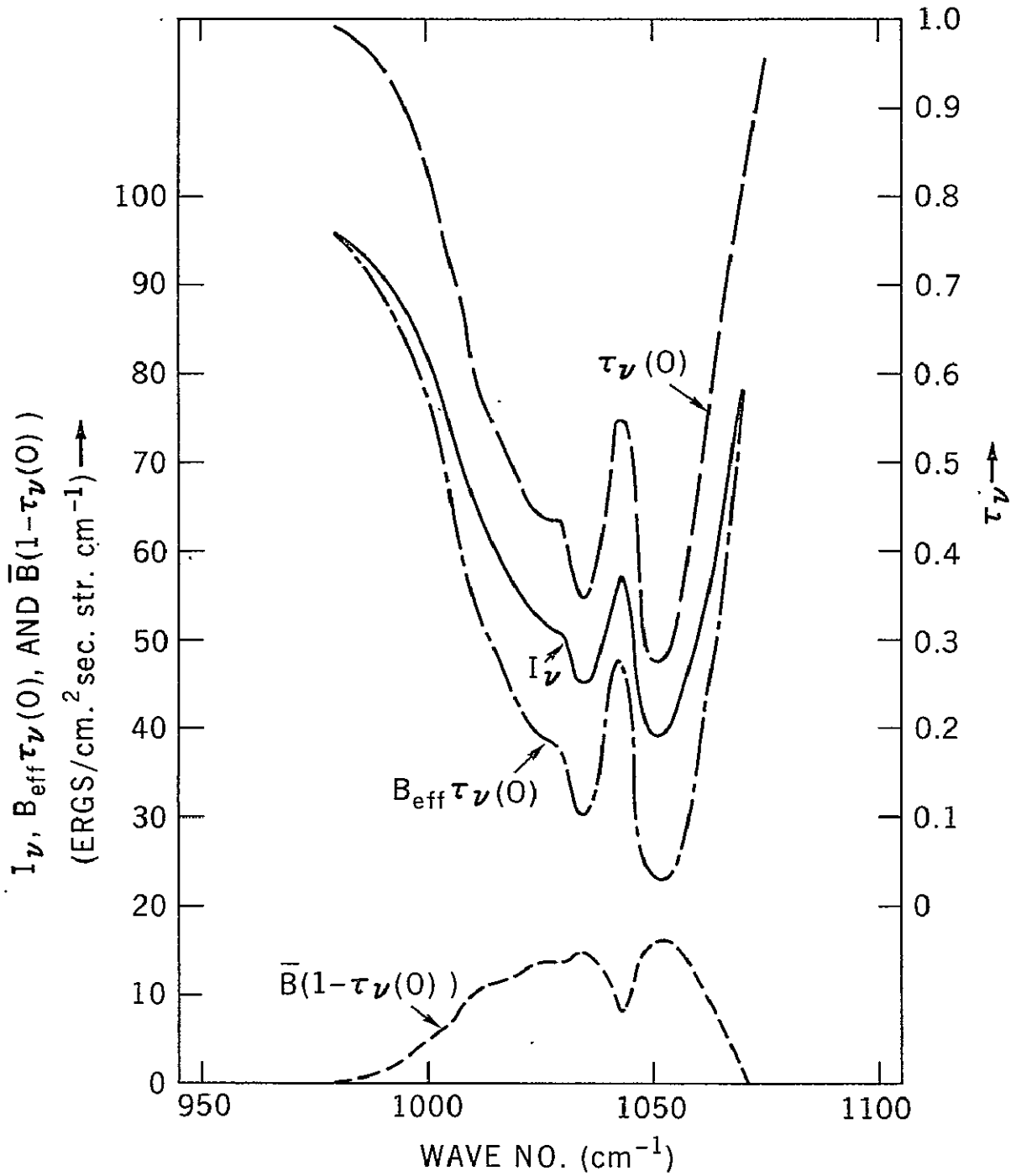


Figure 11—Comparison of the Various Terms in the Equation 13, Corresponding to the Case of Potsdam (June 11, 1969)

computing the synthetic spectrum, are based on the model of Möller and Raschke (1963). The water vapor distribution was such that the troposphere was saturated and the total water content in the atmosphere was 20 gm/cm^2 . The synthetic spectrum resulting from such large water vapor absorption was inverted in two different ways. In one of the full interaction of the water vapor absorption was taken into account while in the other an effective brightness temperature was used to eliminate water vapor interaction. The inverted ozone profiles, from the two ways, agreed closely and the derived total ozone differed only by about 3%. This test justifies the use of effective brightness temperature of the surface.

We have not been able to demonstrate how well our method is functioning in cloudy and partially cloudy situations. It is necessary to make quantitative comparisons in several cloudy situations to resolve this issue.

From the preceding detailed considerations of the various aspects of our inversion method we are inclined to believe that we can determine the atmospheric ozone accurate to within 10% over most of the globe with the exception of polar winter zone where conditions of near isothermal distribution can introduce large errors. Such an accuracy is needed to resolve day to day changes and geographical variations of ozone. A preliminary study of the ozone distribution over the Northern Hemisphere, deduced from IRIS data, lends ample support to this assertion.

ACKNOWLEDGEMENTS

It is a pleasure to thank my colleagues Drs. B. J. Conrath, R. E. Samuelson, V. Kunde, and A. Krueger for several helpful discussions.

The author is grateful to Messrs. W. S. Hering and T. R. Borden of the Air Force Cambridge Research Laboratories, Bedford, Massachusetts, for furnishing data from many chemical soundings. The Canadian Meteorological Service was kind to supply total ozone data.

The service rendered by the personnel at the Wallops Island Meteorological Station and at Point Mugu has enabled the author to make this study quantitative.

Many thanks are due to Mrs. Elsie M. Brookshier for careful typing of the manuscript.

REFERENCES

- Clough, S. A. and F. X. Kneizys (1965), "Ozone Absorption in the 9.0 Micron Region," AFCRL-65-862, Physical Sciences Research Papers No. 170, Air Force Cambridge Research Laboratories, Bedford, Massachusetts, 77 pages.
- Clough, S. A. and F. X. Kneizys (1966), "Coriolis Interaction in the γ_1 and γ_3 Fundamentals of Ozone," The Jour. of Chem. Phys., Vol. 44, No. 5, pp. 1855-1861.
- Conrath, B. J. (1969), "On the Estimation of Relative Humidity Profiles from Medium Resolution Infrared Spectra Obtained from a Satellite," Jour. of Geoph. Res., Vol. 74, pp. 3347-3361.
- Dobson, G.M.B., D. C. Harrison and J. Lawrence (1928), "Measurements of the Amount of Ozone in the Earth's Atmosphere and its Relation to Other Geophysical Conditions," Proc. Roy. Soc. London A, 122, pp. 456-486.
- Goldman, A., D. Murcray, F. Murcray and W. Williams, (1967), "Atmospheric Absorption of Solar Radiation by the 9.6μ Ozone Band," AFCRL-67-0572, Contract AF 19(628)-5202, Scientific Report No. 6., Air Force Cambridge Research Laboratories, Bedford, Massachusetts.
- Hering, W. S., and T. R. Borden (1965), "Mean Distributions of Ozone Density over North America, 1963-1964, AFCRL-65-913, Environmental Research Papers No. 162, Air Force Cambridge Research Laboratories, Bedford, Massachusetts.
- Hering, W. S. and T. R. Borden (1967), "Ozone Sonde Observations Over North America," Vol. 4, AFCRL-64-30(IV), Environmental Research Papers, No. 279., Air Force Cambridge Research Laboratories, Bedford, Massachusetts.
- Holmstrom, I. (1963), "On a Method for Parametric Representation of the State of the Atmosphere," Tellus, Vol. 15, No. 2, pp. 127-149.
- Krueger, A.J. (1969), "Rocket Measurements of Ozone," Annales de Geophysique, Tome 25, pp. 307-311.
- Kunde, V. (1969), Private communication.
- Mateer, C. L., (1965), "On the Information Content of Umkehr Observations," Jour. of the Atmospheric Sciences, Vol. 22, pp. 370-381.

- Moller, F., and E. Raschke (1963), "Evaluation of TIROS III Radiation Data," Interim Report No. 1, NASA Research Grant NSg-305 - Ludwig-Maxmillians-Universität, Meteorologische Institut, Munich, 114 pages.
- Mueller, J. I., (1968), "Ozone Sonde, Bubbler Type," AFCRL-68-0409, Mast Development Comp., Final Report, Project No. 8628, Air Force Cambridge Research Laboratories, Bedford, Massachusetts, 26 pages.
- Prahhakara, C., (1969), "Feasibility of Determining Atmospheric Ozone from Outgoing Infrared Energy," Monthly Weather Review, Vol. 97, pp. 307-314.
- Sekihara, K., and C. D. Walshaw, (1969), "The Possibility of Ozone Measurements from Satellites Using the 1043 cm^{-1} Band," Annales de Geophysique, Tome 25, pp. 233-241.
- Walshaw, C. D., (1954), "An Experimental Investigation of the 9.6μ Band of Ozone," Ph.D. Thesis, Cambridge University, England, 1954, 102 pages.